Measured Multi-User MIMO Capacity in Aircraft

James R. Nagel, Alyssa Magleby Richards, Sai Ananthanarayanan, and Cynthia M. Furse

Department of Electrical and Computer Engineering
University of Utah, Salt Lake City, UT 84112 USA
E-mail: cynthia.furse@utah.edu

Abstract

The multipath richness typical of aircraft channels represents a potentially well-suited environment for multi-user multiple-input multiple-output technology (MU-MIMO). This paper presents results from measurements of the achievable MU-MIMO data rates in a Rockwell T-39 Sabreliner, using an open-source software-defined radio (SDR) test bed. We also compared the achievable capacity of dirty-paper coding (DPC) against time-division multiple access (TDMA) to illustrate the value of advanced MU-MIMO techniques in aircraft environments. Measured data was then compared against values obtained from a three-dimensional ray-tracing simulation. For transmitters located near the ends of the aircraft, the average error between simulated and measured capacity was on the order of 2% or less. For the more-centralized transmitter location, simulations predicted an average of 6% less capacity than what was actually measured.

Keywords: Aircraft; data acquisition; multi-user MIMO; electromagnetic propagation; channel coding; communications channels

1. Introduction

The rapidly growing field of multiple-input multiple-output (MIMO) communications contains a great deal of promise for satisfying the future demands of high-speed data transfer across wireless networks. However, traditional single-user MIMO (SU-MIMO) poses many practical limits to the potential throughput of data in a downlink with many active users. The emergent field of multi-user MIMO (MU-MIMO) is therefore gaining interest for its ability to efficiently transfer data to many independent users at once [1].

Due to its intrinsically rich multipath [2] and potential for many simultaneously active users, the aircraft cabin is possibly a well-suited application for MU-MIMO technology. With the emergence of broadband wireless data access on airline flights, there is naturally an increasing demand for greater data-transfer rates. Wireless data sensors are also seeing an increase in demand for deployment as a means to improve safety and longevity of aircraft [3]. Although there is some data already available with regards to traditional SU-MIMO capacity [4], little work has been done to characterize the aircraft cabin for strictly MU-MIMO. This paper therefore provides the results of measurements inside the cabin of a T-39 Sabreliner as preliminary work for future measurements within the cabins of commercial airliners. The data from these measurements are also used for validation of ray-tracing software under development.

2. System Model

The basic MU-MIMO downlink consists of a base station equipped with M antennas that transmit to a set of $K \leq M$ user terminals. For simplicity, we assume that each user is equipped with N identical receiving antennas. For a given vector $\mathbf{x}$ of complex voltage symbols broadcasted from the base station, the received vector, $\mathbf{y}_k$, at the kth user terminal is given by

$$\mathbf{y}_k = \mathbf{H}_k \mathbf{x} + \mathbf{n}_k . \tag{1}$$

The matrix $\mathbf{H}_k$ denotes an $N \times M$ channel matrix between the base station and user k, with $\mathbf{n}_k$ denoting a vector of independent, identically distributed complex Gaussian noise. For convenience, we shall assume that each element of $\mathbf{n}_k$ has zero mean and unit variance across all users. We also assume that perfect channel state information is available at the transmitter for the sake of computing capacity.

3. Capacity in MU-MIMO

This next section provides a brief overview of two major techniques for implementing a MU-MIMO network. The first

technique represents an ideal implementation with regards to simplicity, while the second represents an ideal implementation for maximizing capacity. Although there are many more available techniques within the literature that could be examined, all of them involve some sort of tradeoff between these two metrics, and therefore tend to fall somewhere between these two extremes.

3.1 Time-Division Multiple Access

The simplest technique for implementing a MU-MIMO network is through time-division multiple access (TDMA). Under this scheme, each user is allotted a unique time window for downloading information, and the entire system is devoted solely to that user. The capacity for user k during the access window is therefore just the well-known water-filling solution for a single user, which is given by

$$C_k = \max_{\mathbf{Q}_k} \log_2 \left| \mathbf{I} + \rho \mathbf{H}_k \mathbf{Q}_k \mathbf{H}_k^H \right|, \tag{2}$$

where $|\cdot|$ denotes the determinant operation. The matrix $\mathbf{I}$ is the $N \times N$ identity matrix, and $\rho = P_s / P_n$ is the average transmitted-symbol-power-to-received-noise ratio. The matrix $\mathbf{Q}_k$ denotes the transmitting correlation matrix for user k, which is subject to two constraints:

$$\mathbf{Q}_k \geq 0$$

and

$$\mathrm{Tr}\{\mathbf{Q}_k\} = P_t,$$

where $P_t = MP_s$ is the total transmitted power. If we now assume that each user is allotted an equal amount of time, then the system capacity under TDMA is given by the average capacity over all k users:

$$C_{TDMA} = \frac{1}{K} \sum_{k=1}^{K} C_k. \tag{3}$$

Although TDMA is relatively simple to implement, it does not provide the maximum-achievable capacity for an MU-MIMO network. The reason for this is the idleness of the other $k-1$ users, who can drastically increase the throughput of the system by receiving their own independent, parallel bit streams. The true capacity for a multi-user network is therefore found by maximizing the sum-rate capacity over all users at once. A known algorithm which achieves this capacity is called *dirty-paper coding* (DPC) [5].

3.2 Dirty-Paper Coding

In order to compute the dirty-paper coding capacity, we must first invoke a duality that exists between the downlink broadcast channel and the uplink access channel [6]. In other words, we must treat the users as those who are transmitting data, while the base station acts as the receiver. Under this context, the matrix $\mathbf{Q}_k$ is defined as the transmitted correlation for user k, and the sum-rate capacity of a MU-MIMO system is computed using the formula

$$C_{DPC} = \max_{\mathbf{Q}_k} \log_2 \left| \mathbf{I} + \rho \sum_{k=1}^{K} \mathbf{H}_k \mathbf{Q}_k \mathbf{H}_k^H \right|. \tag{4}$$

The constraints on the $\mathbf{Q}_k$ matrices are similar to those of the water-filling case, and are given as

$$\mathbf{Q}_k \geq 0$$

and

$$\sum_{k=1}^{K} \mathrm{Tr}\{\mathbf{Q}_k\} = P_t.$$

Computation of this capacity is rather involved, but may be readily achieved by utilizing the algorithms found in [7]. Physical implementation of dirty-paper coding is also computationally intensive, and cannot yet be achieved in real time. Nevertheless, it is still a useful benchmark for characterization, because it represents the absolute highest capacity available.

3.3 Channel Matrix Estimation

A fortunate aspect of channel-capacity measurement is that one need not physically implement a given algorithm in order to calculate its potential capacity. In fact, the only requisite measurement is a set of $\mathbf{H}$ matrices over the various test locations. It is therefore important to understand how a channel matrix is computed from a packet of data.

We begin by defining a complex $M \times L$ matrix $\mathbf{T}$, called the training sequence, and write it as a series of column vectors with the form

$$\mathbf{T} = \left[\mathbf{t}(1) \,|\, \mathbf{t}(2) \,|\cdots|\, \mathbf{t}(L) \right]. \tag{5}$$

In other words, each column vector $\mathbf{t}(\ell)$ represents an $M \times 1$ vector of complex data symbols being broadcast by the transmitter at time ℓ. The $N \times L$ matrix of sampled symbols at the kth receiver may therefore be written as

$$\mathbf{Y}_k = \mathbf{H}_k \mathbf{T} + \mathbf{N}_k, \tag{6}$$

where $\mathbf{N}_k$ is simply an $N \times L$ matrix of sampled noise.

Because $\mathbf{T}$ is a known sequence of data, it can be used to estimate the channel matrix. Defining the matrix $\widetilde{\mathbf{H}}_k$ as the channel-matrix estimate, we may simply write

$$\widetilde{\mathbf{H}}_k = \mathbf{Y}_k \mathbf{T}^+ = \mathbf{H}_k + \mathbf{N}_k \mathbf{T}^+, \tag{7}$$

where $\mathbf{T}^+$ denotes the Moore-Penrose pseudoinverse of $\mathbf{T}$, and is given by

$$\mathbf{T}^+ = \left(\mathbf{T}^H \mathbf{T} \right)^{-1} \mathbf{T}^H. \tag{8}$$

As long as the signal-to-noise ratio (SNR) at the receiver is relatively large, the effects of the noise term $\mathbf{N}_k$ are negligible, and $\widetilde{\mathbf{H}}_k \to \mathbf{H}_k$. The effects of noise may be further reduced by choosing a relatively large value for L. This is because the quantity

$\mathbf{N}_k \mathbf{T}^+$ behaves much like a correlation between the training sequence and the noise. In the limit as $L \to \infty$, we thus have $\mathbf{N}_k \mathbf{T}^+ \to 0$ for uncorrelated noise. So as long as the channel itself remains stationary over the duration of the training sequence, L may be chosen as any arbitrarily large value. For the data presented in this paper, all channel matrices were estimated using a training sequence of pseudo random data with length $L = 4000$.

4. MIMO Test Bed Description

The test bed used to measure data for this paper was a soft-ware-defined radio platform based on the GNU-Radio toolkit [8]. Shown in Figure 1, the equipment was capable of supporting a 4×4 SU-MIMO array at a center frequency of 915 MHz with a sampling rate of 800 kHz. The antenna elements used with this system were quarter-wavelength monopoles, fixed above a 15 in × 18 in ground plane, separated by a distance of one-quarter wavelength (8.2 cm). The average power radiated by each antenna was fixed at approximately 5 mW, thus radiating 20 mW from the entire four-element array. For transmitting locations in close proximity to the receiving array, the output power was cut back to 0.5 mW to prevent saturation of the receivers.

The transmitted data packets were designed around the 4-QAM modulation scheme using differential encoding with 50 kbps of data per antenna. Each packet began with a simple SISO preamble of 4000 pseudorandom data bits, designed to facilitate phase and timing synchronization by the receiver. The packet then transmitted a MIMO sequence of 4×4000 pseudorandom bits to be used as a training sequence for channel estimation. The packet then terminated with a small MIMO payload of text data to verify proper packet detection in post processing.
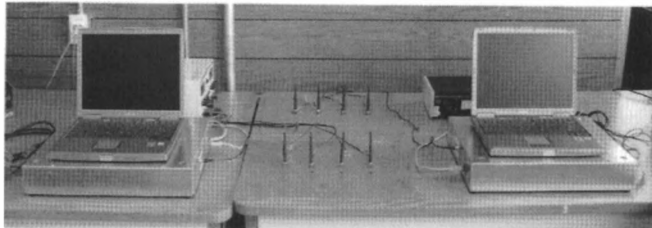

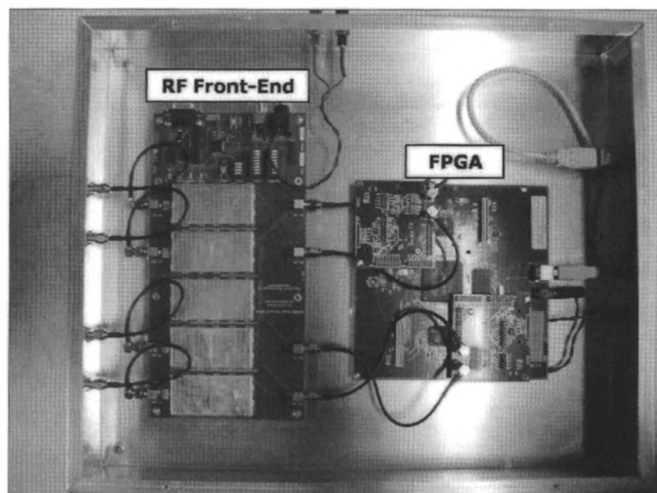Figure 1a. The University of Utah MIMO software-defined-radio test bed.

Figure 1b. An inside view of the chassis with the RF front end and FPGA.
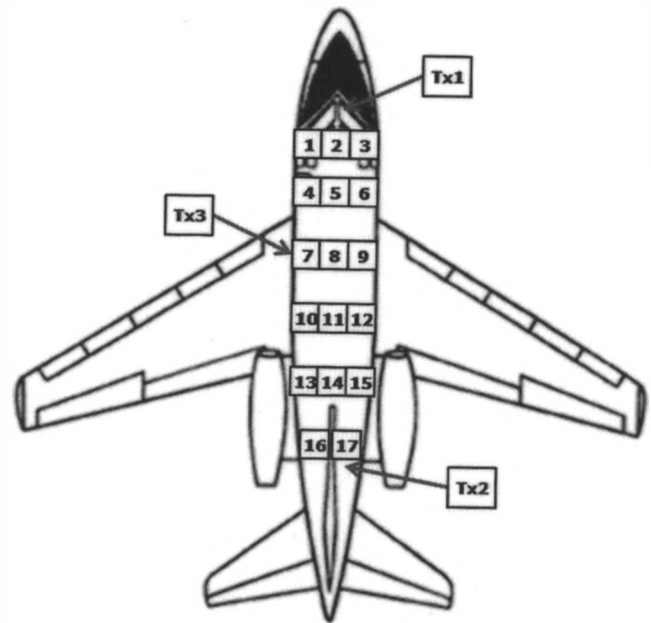

Figure 2. The Rockwell T-39 Sabreliner. Test locations for the receiving array are marked with numbered boxes. The transmitter locations are indicated by the arrows, with Tx1 placed in the dashboard of the cockpit, Tx2 in a maintenance bay in the tail, and Tx3 in a seat near the center of the cabin in place of Rx7.
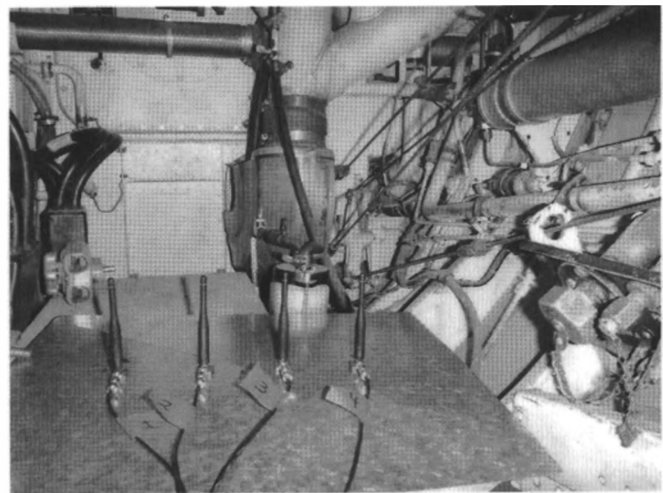

Figure 3. The four-element transmitting array at location Tx2 inside the maintenance bay of the aircraft. The elements were quarter-wavelength monopoles fixed to a conductive ground plane. The elements were separated by a spacing of 8.2 cm, or one-quarter wavelength.

5. Measurement Setup

Measurements were taken in a Rockwell T-39 Sabreliner, which is a typical mid-size commuter aircraft (47 feet from nose to tail). Three transmitter locations were chosen throughout the aircraft, and are depicted in Figure 2. The first location (Tx1) was placed at the center of the dashboard in the cockpit. The second location (Tx2) was placed within a maintenance bay underneath the tail. The third location (Tx3) was placed in a centralized location within the cabin. The receiver locations were chosen to cover the interior of the cabin as uniformly as possible, thus providing a

comprehensive survey of the interior. A mapping of these locations is also shown in Figure 2, and an example deployment within the aircraft is shown in Figure 3.

After placing the receiving array at its specified location, a training packet of data was broadcast by the transmitting array, thereby providing a direct measurement of the channel matrix for that given transmitter/receiver pair. The receiving array was then moved to the next location, where another packet was transmitted. This cycle was then repeated until the survey of the interior was complete. As long as the environment within the cabin remained stationary over the measurement cycle, all channel matrices could be treated as though they were obtained simultaneously. This allowed us to choose any arbitrary permutation of users from the receiving locations and to calculate the multi-user capacity from Equations (3) and (4).

6. Results

6.1 Post Processing

To provide consistency of gain between antennas, all sampled data were normalized to a unit noise variance at each antenna. This was accomplished by isolating an unused portion of the spectrum, and applying the matched filter as if there were actual data. The resultant noise variance was then used as the normalization factor for the antenna. Also, it is common in MIMO measurements to normalize the channel matrices in order to eliminate capacity variations due to path loss. The resultant capacity after normalization is thus a reflection of the relative multipath richness of the channel, rather than any particular gain due to proximity with the transmitter. For our data, all channel matrices were specifically fixed to a unit Frobenius norm. That is to say, $\|\mathbf{H}_k\| = 1$ for all data. Symbol power was then fixed to the arbitrary value of $P_s = 100$, thereby giving an SNR of $\rho = 20$ dB.

For transmitter location Tx1, all 17 of the interior locations were successfully measured, thereby providing a total of $\binom{17}{4} = 2380$ permutations of multi-user locations for statistical analysis. At Tx2, only 11 of the receiver locations could be reliably measured, due to the path loss through the maintenance port[1]. This gave $\binom{11}{4} = 330$ permutations to analyze. For Tx3, only 10 of the receiver locations were successfully measured. This was limited by our test equipment occupying some of the more-centralized locations during the test. The total permutations for this set was therefore $\binom{10}{4} = 210$.

6.2 Measured Capacity

Figure 4 summarizes the results from our measurements by displaying the empirical cumulative distribution functions (CDF)

[1]The loss of signal should not be construed as a physical limitation of the aircraft channel. Rather, our receiver simply lacked a proper low-noise front end, thereby placing significant limits on our sensitivity.

of capacity when calculated using Equations (3) and (4). Clearly, dirty-paper coding offered a substantial gain in capacity over TDMA, thereby illustrating the tremendous advantages of MU-MIMO that have yet to be exploited. We also saw that capacity exhibited very little variability over the permutations of users, as indicated by the relatively tight bounds on the CDF curves. This was indicative of a strong uniformity in multipath richness throughout the cabin. Finally, we saw that Tx3 stood out somewhat from the other two, indicating that a centralized position for the transmitter was marginally preferable when broadcasting to multiple users at once.

6.3 Simulated Capacity

The software we used for simulating the channel matrices was a site-planning ray-tracer that was developed at the University of Hawaii. The algorithm utilized the triangular-grid method [9], and was validated in previous work such as [10]. A screen capture of the GUI is shown in Figure 5, which illustrated our simulation setup. For this paper, we modeled the aircraft fuselage as a faceted, three-dimensional metal cylinder. For the aircraft interior, we inserted reflective and lossy barriers to serve as walls and seats.
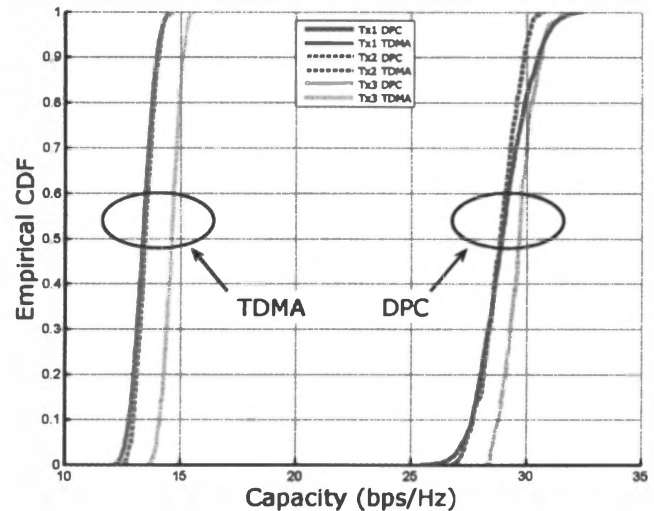

Figure 4. The empirical CDFs of the MU-MIMO capacities under the various permutations of receiver locations. The average SNR was fixed to $P_s/P_n = 20$ dB.
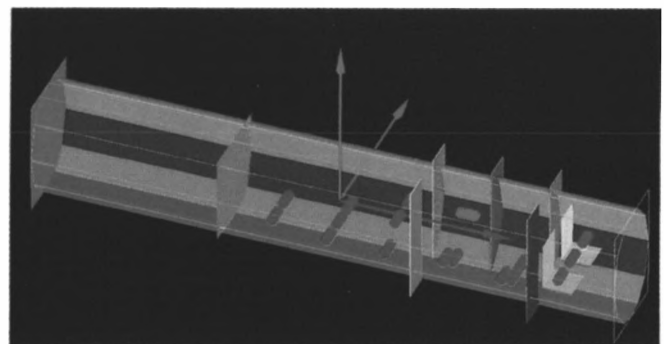

Figure 5. A screen capture of a three-dimensional rendering from the ray-tracing software. The aircraft was modeled as a faceted three-dimensional cylinder with capped ends. The little spheres represent the transmitting and receiving antennas.
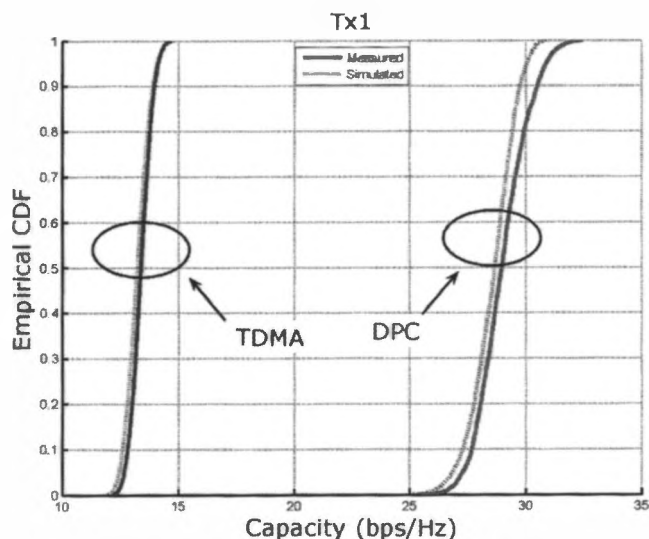
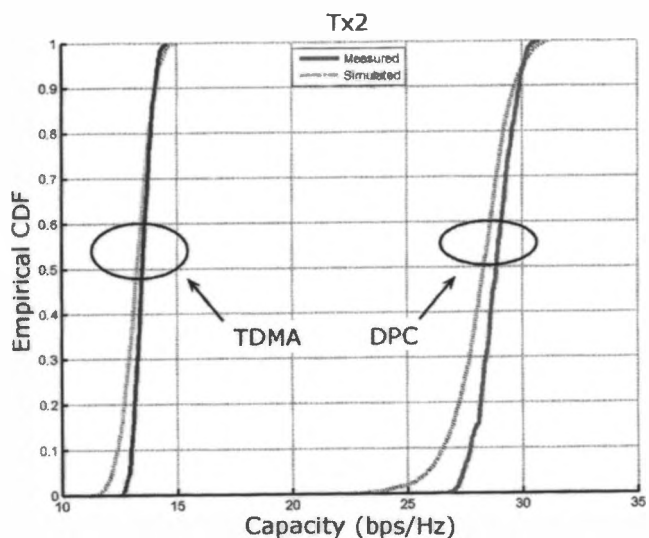**Figure 6. The simulated capacity CDFs compared against measurements, for Tx1.**

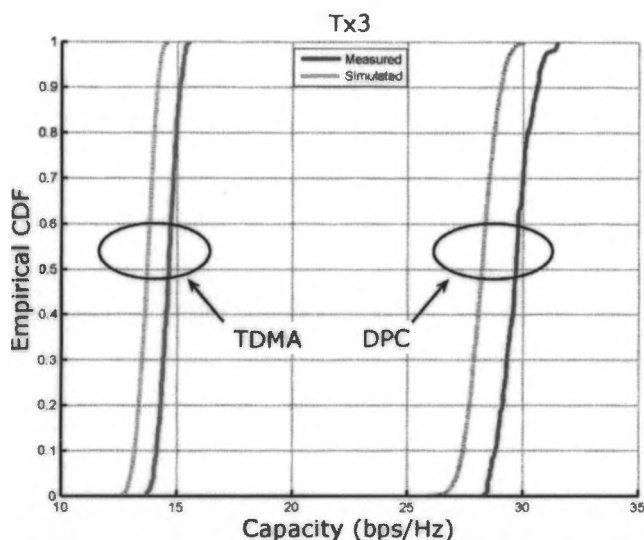**Figure 7. The simulated capacity CDFs compared against measurements, for Tx2.**

Figure 8. The simulated capacity CDFs compared against measurements, for Tx3.

IEEE Antennas and Propagation Magazine, Vol. 52, No. 4, August 2010

Figures 6-8 compare the simulation results against measured capacity for each transmitter location. For Tx1 and Tx2, the mean error between simulation and measurement never exceeded 1.5%. Very similar results could also be obtained by removing all interior walls from the cabin. This indicated to us that the vast majority of multipath richness in these two scenarios was due entirely to reflections off the fuselage itself, and had very little to do with the interior features, such as walls and chairs. However, for Tx3 the simulations tended to predict lower capacity than what was actually measured, with errors on the order of 5%-6%. This was a surprising result, as it indicated that multipath richness near the center of the aircraft was most likely the result of reflective structures near the transmitter, and not the exterior walls alone.

7. Conclusions

This paper presented measurement data for MU-MIMO capacity in a Rockwell T39 Sabreliner. Channel statistics were gathered by utilizing the various permutations of users within our measured data sets to provide a comprehensive survey of possible user arrangements within the cabin. We have shown that capacity under dirty-paper coding is much greater than with TDMA, thereby indicating the gains in throughput that have yet to be exploited in the aircraft channel. We have also shown how normalized capacity is fairly independent of the spatial distribution of users, indicating a relative uniformity of multipath richness throughout the cabin. We then presented a comparison of these measurements against ray-tracing simulation results. The results indicated that the ray-tracer was capable of predicting multipath richness within 2% of the measurements when the transmitters were located at the ends of the cabin, and 6% when centralized.

8. Acknowledgments

9. References

1. Q. H. Spencer, C. B. Peel, A. L. Swindlehurst, and M. Haardt, "An Introduction to the Multi-User MIMO Downlink," *IEEE Communications Magazine*, **42**, October 2004, pp. 60-67.

2. C. Fitzhugh, J. Frolik, J. Covell, R. Ketcham, and T. Meyer, "2.4 GHz multipath environments in airframes," the 2005 IEEE Annual Conference on Wireless and Microwave Technology, 2005, WAMICON 2005, Clearwater, FL, April 2005.

3. P. R. SaiAnanthanarayanan, A. Magleby, J. R. Nagel, and C. Furse, "MIMO Wireless Communication for Aircraft Sensors," 12th Joint FAA/DOD/NASA Conference on Aging Aircraft, Kansas City, May 2009.

4. R. W. H. Bhagavatula, Jr., and S. Vishwanath, "Optimizing MIMO Antenna Placement and Array Configurations for Multimedia Delivery in Aircraft," IEEE 65th Vehicular Technology Conference, Dublin, Ireland, April 2007, pp. 425-429.

5. H. Weingarten, Y. Steinberg, and S. S. Shitz, "The Capacity Region of the Gaussian MIMO Broadcast Channel," Proceedings of the IEEE International Symposium on Information Theory (ISIT2004), March 2004, p. 174.

6. S. Vishwanath, N. Jindal, and A. Goldsmith, "Duality, Achievable Rates, and Sum-Rate Capacity of Gaussian MIMO Broadcast Channels," *IEEE Transactions on Information Theory*, **49**, October 2003, pp. 2658-2668.

7. N. Jindal, W. Rhee, S. Vishwanath, S. A. Jafar, and A. Goldsmith, 'Sum Power Iterative Water-Filling for Multi-Antenna Gaussian Broadcast Channels," *IEEE Transactions on Information Theory*, **51** April 2005, pp. 1570-1580.

8. D. Palchak and B. Farhang-Boroujeny, "A Software Defined Radio Testbed for MIMO Systems," Proceedings of the SDR 06 Technical Conference and Product Exposition, Orlando, FL, November 2006.

9. Z. Yun, Z. Zhang, and M. F. Iskander, "A Ray-Tracing Method Based on the Triangular Grid Approach and Application to Propagation Prediction in Urban Environments," Proceedings of the IEEE International Symposium on Information Theory (ISIT2004), **50**, May 2002, pp. 750-758.

10. S. Y. Lim, Z. Yun, J. M. Baker, N. Celik, H.-S. Youn, and M. F. Iskander, 'Radio Propagation in Stairwell: Measurement and Simulation Results," IEEE International Symposium on Antennas and Propagation, Charleston, SC, June 2009.